ELSEVIER

Contents lists available at ScienceDirect

Mechanics of Materials

journal homepage: www.elsevier.com/locate/mechmat



Research paper

Improved approximation of transverse and shear stiffness for high volume fraction uniaxial composites



J. Morris, Christopher J. Hansen, Alireza V. Amirkhizi*

Department of Mechanical Engineering, University of Massachusetts, Lowell, One University Avenue, Lowell, MA 01854, United States

ARTICLE INFO

Keywords: Uniaxial fiber-reinforced composites Shear moduli Transverse moduli Micromechanics Periodic composites Fiber interaction Experimental validation

ABSTRACT

With uniaxial composites, the matrix material properties dominate the overall transverse and shear composite stiffness. Knowledge of these quantities are of practical importance in composite structures such as large wind turbine blades, which despite having a predominantly uniaxial layup, have both their torsional response and buckling behavior as critical design considerations. Accurate estimations of transverse and torsional rigidity for high volume fraction composites are currently dependent on extensive experimental work due to the low reliability and precision of transverse/shear micromechanical models. The Continuous Periodic Fiber Model is proposed to improve these predictions by considering fiber-fiber interactions through the use of periodic boundary conditions. Experimental data and standard models are used to validate the results and quantify the predictive improvements relative to traditional methods. The Continuous Periodic Fiber Model offers greatly improved accuracy for transverse stiffness estimations, reducing the average difference from the experiments by a factor of 1.7 (an average difference with experiment of 14% compared to the next best approach value of 24%) as well as modest improvements for the shear moduli.

1. Introduction

Composite materials, such as fiberglass or carbon fiber-reinforced polymer, consist of a stiff fiber reinforcement infused with a more compliant resin matrix. The reinforcement material provides enhanced stiffness along its primary axis (fiber orientation), but the response of the lamina off-axis is heavily dependent on the matrix material used. More specifically, the matrix material dominates the lamina transverse and shear properties. In most engineering applications the composite laminates consist of layups of laminae with fiber axes oriented in multiple directions, such that the effect of the transverse properties of a single lamina on the overall behavior of the composite is overshadowed by the axial properties of other plies. However, in certain large structures such as wind turbine blades, a significant portion of the plies comprising the composite structure are uniaxially orientated. Moreover, blade structural failures due to buckling and trailing edge splitting are especially sensitive to its transverse and torsional rigidity Schubel and Crossley (2012); Eder and Bitsche (2015); Griffith and Ashwill (2011).

Efforts to optimize the resin/composite performance are reliant on having a high fidelity micromechanical model that can accurately characterize the matrix contribution. The transverse and shear properties are notoriously difficult to approximate for high volume fraction

uniaxial composites due to the increased contribution of matrix-fiber inter-facial strength and fiber-fiber interactions; see for example Hyer (1998). Based on the pioneering work by Nemat-Nasser and his coworkers Iwakuma and Nemat-Nasser (1983); Nemat-Nasser and Hori (1993); Nantasetphong et al. (2016), an advanced micromechanical method called the Continuous Periodic Fiber Model (CPFM) was developed that incorporates the effects of fiber-fiber interactions through Fourier series expansions of the periodic fiber distribution. Using a collection of experimental data for fiberglass composite systems, the accuracy of this advanced model was validated. For perspective, the CPFM approximations were then compared to approximations from three widely adopted models.

2. General assumptions

The micromechanical models used in this work include two variations of the Rule of Mixtures (ROM) method, the Composite Cylinder Model (CCM), and the Continuous Periodic Fiber Model (CPFM). Individual material assumptions for the matrix, fiber, and composite are generally consistent between models.

The CPFM method utilizes a square repeating unit cell (RUC) with periodic boundary conditions. CPFM has been developed using the square cell to minimize the complexity of the calculations, though the

E-mail address: alireza_amirkhizi@uml.edu (A.V. Amirkhizi).

^{*} Corresponding author.

formulations can be expanded to incorporate a hexagonal array. Generally, the former is considered to be a less realistic representation of the way the fibers would naturally align themselves at higher values of volume fraction, where rather than settling in neat square rows and columns, the round fibers would more realistically align themselves in a triangular or hexagonal pattern.

Individually, the matrix and fibers are considered isotropic, although this is not a requirement for CPFM. Fiber anisotropy will require minor modifications to the CPFM approach as it is discussed here, while potential matrix anisotropy requires recalculation of the periodic Eshelby tensor introduced in Section 3.

In the following the Voigt notation is used, in which symmetric tensors are represented as 6×1 vectors instead of 3×3 matrices. Furthermore, the strain vector uses engineering shear strain quantities. The 4th order elasticity tensor can therefore be represented by a symmetric 6x6 matrix. For example, orthotropic elasticity is written in Voigt notation as

$$\begin{pmatrix}
\tau_{1} = \sigma_{11} \\
\tau_{2} = \sigma_{22} \\
\tau_{3} = \sigma_{33} \\
\tau_{4} = \sigma_{23} \\
\tau_{5} = \sigma_{13} \\
\tau_{6} = \sigma_{12}
\end{pmatrix} = \begin{pmatrix}
C_{11} & C_{12} & C_{13} & 0 & 0 & 0 \\
C_{12} & C_{22} & C_{23} & 0 & 0 & 0 \\
C_{13} & C_{23} & C_{33} & 0 & 0 & 0 \\
0 & 0 & 0 & C_{44} & 0 & 0 \\
0 & 0 & 0 & 0 & C_{55} & 0 \\
0 & 0 & 0 & 0 & C_{66}
\end{pmatrix} \times \begin{pmatrix}
\gamma_{1} = \varepsilon_{11} \\
\gamma_{2} = \varepsilon_{22} \\
\gamma_{3} = \varepsilon_{33} \\
\gamma_{4} = 2\varepsilon_{23} \\
\gamma_{5} = 2\varepsilon_{13} \\
\gamma_{6} = 2\varepsilon_{12}
\end{pmatrix}$$
(1)

The unidirectional laminate being approximated is always assumed to be orthotropic, where the properties along the fiber length (1) are distinct from the in-plane transverse direction (2) and out-of-plane normal direction (3). The values of the orthotropic moduli may always be calculated from considering the compliance tensor written in 6 by 6 matrix with Voigt's notation:

$$[C]^{-1} = [S] = \begin{bmatrix} 1/E_1 & -\nu_{12}/E_1 & -\nu_{13}/E_1 & 0 & 0 & 0 \\ -\nu_{12}/E_1 & 1/E_2 & -\nu_{23}/E_2 & 0 & 0 & 0 \\ -\nu_{13}/E_1 & -\nu_{23}/E_2 & 1/E_3 & 0 & 0 & 0 \\ 0 & 0 & 0 & 1/G_{23} & 0 & 0 \\ 0 & 0 & 0 & 0 & 1/G_{31} & 0 \\ 0 & 0 & 0 & 0 & 0 & 1/G_{12} \end{bmatrix}.$$
(2)

3. Continuous periodic fiber model (CPFM)

3.1. Background

In his highly celebrated work, Eshelby (1957) developed a model that could account for the spontaneous phase change of an ellipsoidal inclusion within an infinite matrix domain. His work has found tremendous application, as the aspect ratios of an ellipsoid can be changed to approximate a variety of geometries, including practical cases with inclusions such as spherical beads, flat disks or platelets, and long thin continuous fibers.

Nemat-Nasser et al. (1982) applied periodic boundary conditions to a repeating unit cell and its eigenstrain fields following Eshelby's work. These boundary conditions led to a Fourier series solution for the effective bulk and shear moduli of the systems that could be improved by increasing the number of terms. Their comparisons with experimental results for sintered alumina, sintered perlite, and porous glass with inclusion volume fractions up to 50% demonstrated excellent correlation. The approach of expanding the periodic parts of field quantities using Fourier series was also discussed by Mura (1987).

Iwakuma and Nemat-Nasser (1983) presented a more general solution for periodic structures, outlining the procedure for determining the overall properties of a composite with ellipsoidal inclusions of any aspect ratio. They define the periodic version of Eshelby's tensor as S^P , whose components are dependent only on the geometry of the inclusion and the Poisson's ratio of the isotropic matrix. Their final solution is written in terms of the matrix elasticity, inclusion elasticity, inclusion

volume fraction, and ellipsoidal inclusion aspect ratio. Nemat-Nasser and Hori (1993) collected their works into a book which features an expansion of the periodic method. Step-by-step processes for determining the overall properties of composites with assorted geometric configurations are clearly presented, making this work an essential reference for applying their method in practice or building upon it in future works. Their text explicitly addresses cavities, cracks, and inclusions with aspect ratios suitable for application to spheres, platelets, ellipsoids, and long fibers.

From Nemat-Nasser and Hori (1993), as well as Iwakuma and Nemat-Nasser (1983), a periodic model for the transverse modulus similar to the Continuous Periodic Fiber Model (CPFM) presented here was produced by Luciano and Barbero (1994). Their approach differs in that it explicitly separates the matrix elasticity from the transformation tensor. They compare their results to the method of cells (Aboudi, 1996) and a small set of experimentally obtained moduli for a glass-epoxy system. Their work matched closely with the experiments, suggesting that periodic models can accurately capture the complex elastic behavior of high volume fraction composites.

Nantasetphong et al. (2016) applied a periodic method to ellipsoidal glass inclusions within a polyurea matrix. The micromechanical models they developed were validated for dilute periodic media (volume fraction, $V^f \le 20\%$) with randomly oriented and plane-aligned inclusions with aspect ratios of $L/d \approx 10$. To estimate the overall response of a composite with a specific distribution of inclusion orientations, they used a Taylor averaging scheme (in 3D random and plane-aligned distributions). The determined moduli are based on a single periodic unit cell of an aligned inclusion array. CPFM, described in this paper, is a direct adaptation of the Nantasetphong et al. periodic method, specialized to suit an ellipsoidal aspect ratio representing continuous fiber bundles that are axially aligned $(L/d \approx \infty)$. For this reason, no Taylor averaging is required at this stage. The results are compared to the coupon level test data after application of Classical Laminate Theory (described in Section 4) to average the elasticity tensor components over the complete layup. This adjustment also allows the model to maintain its accuracy when applied to high volume fraction composites $(V^f \ge 50\%).$

3.2. Fourier series expansion of the field variables

The Continuous Periodic Fiber Model is formulated through a traditional derivation of the effective elasticity tensor for a composite with periodic boundary conditions on the unit cell. When a uniform macrostrain ε^0 is prescribed to the boundary of the unit cell, the average strain over this domain, $\bar{\varepsilon}$, will match the applied strain $\bar{\varepsilon} = \varepsilon^0$. The overall constitutive elasticity tensor of the composite \bar{C} is calculated based on the average stress over the combined fiber and matrix portions. The elasticity tensors for the matrix (C) and fiber (C^{Ω}) are known. These tensors are determined from the isotropic components E, ν , and C with Eq. (2).

The first step in the derivation of CPFM is to replace the inclusion with an eigenstrain in order to use the homogeneous field equations for the heterogeneous medium, i.e., finding $\varepsilon^*(x)$, such that

$$C'(x): \varepsilon(x) = C: \{\varepsilon(x) - \varepsilon^*(x)\}. \tag{3}$$

The left side of this consistency condition describes the stress state of a heterogeneous cell, where the cell elasticity C'(x) has matrix properties in the matrix domain M and inclusion properties in the inclusion domain Ω . Both strain and stress states of the homogenized cell on the right hand side must be consistent with those of the heterogeneous cell. The right side of the consistency condition assumes both matrix and inclusion domains have the same matrix elasticity tensor, C, so an eigenstrain is introduced to adjust for the presence of the inclusion. In the rest of this section, the strain field in the homogenized cell due to any eigenstrain distribution is calculated.

The periodicity of the cell allows the application of Fourier series

expansions to the strain and displacement fields within the cell. The 3-dimensional periodicity of the model is represented in the summation vector ξ (written in terms of the cell width a_i and element number n_i) for each of the 3 directions in which one desires to consider the interaction of the inclusions:

$$\xi_i = \frac{n_i \pi}{a_i}, \qquad i = 1, 2, \text{ or } 3.$$
 (4)

The Fourier series of the field functions are written as summations over the full range of ξ and integrated over the full volume of the cell U. This integration applies to all non-zero values of ξ . The general form of the Fourier series expansion is:

$$f(\mathbf{x}) = \sum_{\xi} \mathbf{F} f(\xi) e^{i\mathbf{x}.\xi},\tag{5}$$

where

$$Ff(\xi) \equiv \frac{1}{U} \int_{U} f(x) e^{-ix.\xi} dV_{x}$$
(6)

and the superscript Σ' indicates that the summation is made over only the nonzero values of ξ .

The Fourier series expansion of the strain field is written based on the symmetric parts of the displacement gradient tensor:

$$\varepsilon(\mathbf{x}) = \sum_{\xi}' \mathbf{F} \varepsilon(\xi) e^{i\mathbf{x}.\xi} \tag{7}$$

where

$$F\varepsilon(\xi) \equiv \frac{i}{2} \{ \xi \otimes Fu(\xi) + Fu(\xi) \otimes \xi \}.$$
 (8)

Similarly, the eigenstrain is written with a Fourier series expansion to model the effect of repeating inclusion geometries.

$$\varepsilon^*(\mathbf{x}) = \sum_{\xi}' \mathbf{F} \varepsilon^*(\xi) e^{i\mathbf{x}.\xi},$$
(9)

where

$$F\varepsilon^*(\xi) \equiv \frac{1}{U} \int_U \varepsilon^*(\mathbf{x}) e^{-i\mathbf{x}\cdot\xi} dV_{\mathbf{x}}.$$
 (10)

3.3. Periodic Eshelby's tensor

A linear relationship between the strain and eigenstrain is enforced using a fourth order tensor, S^P , that is similar to Eshelby's Tensor. S^P can be written in the spatial domain with index form as it is used by Eshelby (1957)

$$\varepsilon_{ij} = S_{ijkl}^P \varepsilon_{kl}^*,\tag{11}$$

or in the Fourier tensorial form as it is being applied here:

$$F\varepsilon(\xi) = FS^{P}(\xi): F\varepsilon^{*}(\xi). \tag{12}$$

In order to formulate S^P , the displacement and stress field variables must also be expanded. To calculate the average stress over the fiber and matrix portions, consider Hooke's law:

$$\varepsilon = C^{-1}: \sigma + \varepsilon^*, \tag{13}$$

$$\sigma = C: (\varepsilon - \varepsilon^*). \tag{14}$$

Considering the stress equilibrium, ∇ . $\sigma = 0$, Eq. (14) can be expanded and solved for the displacement when $\xi \neq 0$,

$$\nabla. \ \sigma = \nabla(C: (\nabla \otimes u)) - \nabla: (C: \varepsilon^*) = 0, \tag{15}$$

$$i(\xi, C, \xi): Fu(\xi) = \xi. (C: F\varepsilon^*(\xi)), \tag{16}$$

$$Fu(\xi) = -i(\xi, C, \xi)^{-1}.(\xi, (C; F\varepsilon^*(\xi))).$$
 (17)

The coefficient of the periodic Fourier series expansion FS^P can now

be solved for by substituting the displacement field (17) into the Fourier series expansion of the strain (8). Comparing this result to the linear relationship in Eq. (12) gives the definition of $FS^P(\xi)$ as

$$FS^{P}(\xi) = sym\{\xi \otimes (\xi. C. \xi)^{-1} \otimes \xi\}: C.$$
(18)

A more detailed derivation of the strains and displacement fields adjusted for the prescribed eigenstrain, as well as eigenstress, may be found in Nemat-Nasser and Hori (1993).

All terms in FS^P components are known and Eq. (18) is solvable. Before applying it to CPFM, a formatting of FS^P derived by Nemat-Nasser et al. (1982) is considered to reduce the complexity of the solution. The formula for FS^P is split into sub-terms FS^1 , FS^2 , and FS^3 , which are functions of only the unit cell geometry. As for material dependencies, the isotropic matrix elasticity is extracted and simplified such that the terms include only the matrix Poisson's ratio. Note that the solution is completely independent of the inclusion elasticity.

$$FS^{p}(\xi) = FS^{1}(\xi) - \frac{1}{1-\nu}FS^{2}(\xi) + \frac{\nu}{1-\nu}FS^{3}(\xi),$$
 (19)

where the geometric components are defined with the normalized unit vectors $\bar{\xi} = \xi/\xi$ as

$$FS^{1}(\xi) = 2sym(\overline{\xi} \otimes 1^{(2)} \otimes \overline{\xi}). \tag{20}$$

$$FS^2(\xi) = \overline{\xi} \otimes \overline{\xi} \otimes \overline{\xi} \otimes \overline{\xi}$$
 (21)

$$FS^3(\xi) = \overline{\xi} \otimes \overline{\xi} \otimes 1^{(2)}$$
. (22)

3.4. Determination of the strain fields

In order to determine the perturbation from uniform field quantities due to the presence of the heterogeneous inclusion as a function of the homogenizing eigenstrain, the consistency condition is written again, separating the periodic disturbance in the strain, symbolized as ε^p , from the average (applied) strain.

$$C^{\Omega}: \{ \varepsilon^0 + \varepsilon^p(x) \} = C: \{ \varepsilon^0 + \varepsilon^p(x) + \varepsilon^*(x) \}$$
 (23)

In general, this equation can be solved as an integral equation using the results of the previous section. However, only the overall properties are of interest. One approach is to average this version of the consistency condition over the inclusion and solving for the average inclusion strain in terms of the average eigenstrain,

$$\overline{\varepsilon}^{\Omega} = \varepsilon^{0} + \overline{\varepsilon}^{p} = -(C^{\Omega} - C)^{-1} : C : \overline{\varepsilon}^{*}.$$
 (24)

Considering Eq. (12), one can introduce the one and only approximation step in this process by assuming the eigenstrain field may be replaced by its average over the inclusion domain Ω to obtain

$$\varepsilon^{p}(\mathbf{x}) = \left\{ \sum_{\xi}' V^{f} g(-\xi) \mathbf{F} S^{p}(\xi) e^{i\xi \cdot \mathbf{x}} \right\} : \overline{\varepsilon}^{*}$$
(25)

where

$$g(\xi) = \frac{1}{\Omega} \int_{\Omega} e^{-i\xi \cdot x} dV_x \tag{26}$$

is a purely geometric function. To calculate the overall properties, only average values of the perturbation strains are needed and therefore the approximation presented in Eq. (25) (using average eigenstrain and solving the linear system of equations) yields excellent results. The fiber volume fraction $V^f = \Omega/U$ is introduced when the inclusion consistency condition is integrated over each inclusion in the Fourier domain (for all $\xi \neq 0$). The periodic Eshelby's tensor S^P can now be estimated as

$$S^{P} = \sum_{\xi}' V^{f} g(-\xi) g(\xi) F S^{P}(\xi).$$
(27)

Eq. (25) can then be rewritten using this definition of the average

perturbation strain (over the inclusion) as

$$\frac{1}{\Omega} \int_{\Omega} \varepsilon^{p}(\mathbf{x}) dV_{\mathbf{x}} = S^{p}(\xi) : \bar{\varepsilon}^{*}$$
(28)

Note that $g(\xi)$ and $g(-\xi)$ are complex conjugates so their product generates a tensor with real values. This reduced relationship for the average periodic strain disturbance is substituted into the averaged consistency condition (23) over the inclusion to arrive at

$$C^{\Omega}$$
: $\{\varepsilon^0 + S^P : \bar{\varepsilon}^*\} = C$: $\{\varepsilon^0 + (S^P - 1^{(4s)}) : \bar{\varepsilon}^*\}$. (29)

Solving this equation will provide a tensorial relationship between the average eigenstrain, $\tilde{\epsilon}^*$, and average (applied) strain:

$$\bar{\varepsilon}^* = -((C^{\Omega} - C)^{-1}: C - S^P)^{-1}: \varepsilon^0$$
(30)

3.5. Constructing the elasticity tensor

A traditional derivation of the composite effective elasticity tensor is usually based on stress partitioning

$$\bar{C}: \varepsilon^0 = C: \varepsilon^0 + V^f(C^\Omega - C): \bar{\varepsilon}^\Omega.$$
(31)

The average strain in the fiber/inclusion $\bar{\epsilon}^{\Omega}$ is linearly related to the applied strain, $\bar{\epsilon}^{\Omega} = P^f \colon \epsilon^0$, defining the transformation tensor P^f . This relationship is used to eliminate the strain terms from the elasticity equation, leaving only P^f , fiber volume fraction, and the independent matrix/fiber stiffness properties

$$\bar{C} = C + V^f(C^{\Omega} - C): P^f. \tag{32}$$

The transformation tensor P^f is determined for a periodic, cylindrical, axially aligned, short fiber by combining Eqs. (24) and (30) to reflect the linear relationship $\bar{\epsilon}^{\Omega} = P^f$: ϵ^0 . Solving this combined formulation for P^f and substituting it into Eq. (29) leads to a useful formulation for the overall elasticity tensor

$$P^{f} = (C - C^{\Omega})^{-1} : C : ((C - C^{\Omega})^{-1} : C - S^{P})^{-1},$$
(33)

$$\bar{C} = C: \{1^{(4s)} - V^f((C - C^{\Omega})^{-1}: C - S^p)^{-1}\}.$$
(34)

With the knowledge of the periodic Eshelby's tensor, Eq. (34) can be used to calculate the overall composite elasticity. It is important to point out that, using this method, the effective elasticity tensor is exactly the inverse of the effective compliance tensor. This would permit the same solution to be generated by instead calculating the compliance tensor using eigenstress method and an applied stress approach. The details of this approach may be found in Nemat-Nasser and Hori (1993).

4. Classical laminate theory (CLT)

The composites used to obtain the experimental data contained approximately 5% of their structural fibers in the transverse direction for handling stability (along with minimal through thickness stitching). To permit a more precise analysis of composites with various layups, Classical Laminate Theory (CLT) and in-plane rotation of unidirectional lamina is used. Hyer (1998) outlines the methodology for determining the moduli of a unidirectional laminate loaded along ply angles that are rotated between the axial and transverse orientations.

For purely in-plane problems, the terms of the elasticity tensor that define the material response to axial, transverse, and in-plane shear strains may be constructed based on Voigt notation for any in-plane rotation:

$$[Q'_{ij}] = [T_1]^{-1} \begin{bmatrix} C_{11} & C_{12} & 0 \\ C_{12} & C_{22} & 0 \\ 0 & 0 & C_{66} \end{bmatrix} [T_2].$$
(36)

where $[T_1]$ and $[T_2]$ are the rotations matrices associated with stress and strain, respectively, and are determined as functions of the ply angle θ :

$$m = \cos \theta, \qquad n = \sin \theta \tag{37}$$

$$[T_1] = \begin{bmatrix} m^2 & n^2 & 2mn \\ n^2 & m^2 & -2mn \\ -mn & mn & m^2 - n^2 \end{bmatrix}$$
(38)

$$[T_2] = \begin{bmatrix} m^2 & n^2 & mn \\ n^2 & m^2 & -mn \\ -2mn & 2mn & m^2 - n^2 \end{bmatrix}.$$
 (39)

A separate elasticity tensor, $[Q_{ij}^{(p)}]$, can be produced for each ply angle in the layup. In the following it is assumed that the fiber volume fraction is the same in all plies but the areal weight fraction of all of the plies along a prescribed fiber angle is f_p . After the averaging/integration of the elasticity tensors, the compliance is calculated by matrix inversion and then the individual terms of the compliance are taken to determine the effective engineering properties of the composite.

$$[S] = [C]^{-1} = \left[\sum_{p=1}^{n} f_p[Q_{ij}^{\prime p}]\right]^{-1},\tag{40}$$

For systems that are not primarily uniaxial, the CLT approach alone provides reasonable estimates for the transverse modulus, even with an inaccurate transverse modulus for the uniaxial lamina, due to the fact that the overall response of most layups that are not primarily uniaxial, are dominated by the lamina modulus in the direction along the fibers. By contrast, in applications such as wind turbine blade design, the use of primarily uniaxial layups makes proper estimation of the transverse properties significant.

5. Model validation and comparison with experimental data

The usefulness of a micromechanical model relates to its ability to accurately and consistently produce a result that closely corresponds to real world applications. A statistically significant database of measured material properties, generally collected from coupon level experiments, is necessary in order to prove the effectiveness and range of a newly developed methodology to an acceptable level of confidence. However, a compatible set of axial, transverse, and shear measured elastic properties for unidirectional composites is time-consuming and costly to obtain.

In this study, the experimental data used for validation consists of 253 individual property measurements for 7 distinct fiberglass material systems and was graciously provided by TPI Composites. They provided a robust set of statistical data for each material system which averages variations between laminates and samples within the same laminate. The testing standards included ISO 527-5 for the axial/transverse tension measurements and ASTM D7078 for shear. While the data set was mostly complete, a compatible set of three properties was not available for all material systems. The experimental standard deviations ranged from 1–7%, so a target for micromechanical model accuracy of around 7% would provide accuracy on par with what can be measured physically.

The calculated composite volume fractions in these comparisons varied slightly between each laminate and range from 54–58% fiber content. The CLT methodology discussed in Section 4 was used to apply the layup correction to the predicted unidirectional properties in order to account for the 5% transverse stabilizing fibers when comparing to experimental data. The small amount of through thickness stitching fibers are ignored in this study.

The results for the CPFM model and commonly used traditional models are presented with the experimental dataset so that the advantages and discrepancies of each model as compared with the experimental data can be evaluated. The traditional models considered include the most basic form of the Rule of Mixtures method (ROM) (Voigt, 1889; Reuss, 1929; Hyer, 1998), a more complex form of the Rule of Mixtures that incorporates the Poisson's effect (ROMc) (Hyer, 1998), and the Composite Cylinder Model (CCM) (Hill, 1963; Hashin, 1966; Christensen and Lo, 1979). All these standard models give a transversely isotropic elasticity tensor for the lamina. In contrast, CPFM gives an orthotropic result with matching properties in 2 and 3 directions. While a Taylor averaging scheme may be used to get an estimated transversely isotropic tensor based on CPFM, this procedure is not used here. It is intuitively expected to observe an orthotropic response in lamina, since the through thickness direction is physically different the in-plane. The resin pockets (potentially with plane-like geometry) between woven fiber sheets tend to reduce the throughthickness stiffness significantly, while in contrast the average in-plane spacing of the fibers should be less than expected from a simple square packed array considered in this realization of CPFM. Ultimately, the CPFM orthotropic results are used in the following analysis without any changes, as a reasonable estimate in the absence of detailed knowledge of directionality in the resin distribution and fiber-to-fiber spacing. In all cases, the model inputs include the isotropic fiber/resin properties (Young's modulus, Poisson's ratio, shear modulus), fiber volume fraction, and layup distribution for each fiberglass system. The elastic properties of the reinforcement were not made available from the manufacturers, so standard properties of E-glass fibers were used for all of the material systems. The elastic properties of the matrix materials were available from the manufacturer's data sheet for each specific resin.

The experimental results and average predicted moduli values for each of the 7 distinct material systems are plotted as functions of fiber volume fraction in Fig. 1. Each experimental data point represents the average of the specimen modulus values measured for each distinct material systems. All of the modulus results are normalized by the compatible modulus of the resin used to manufacture the specific

Table 1Accuracy of the micromechanical models as defined by the averaged difference from the experimentally obtained properties provided by TPI Composites.

Model	E_1	E_2	G_{12}
ROM	5 ± 7%	41 ± 4%	38 ± 4%
ROMc	5 ± 7%	36 ± 4%	38 ± 4%
CCM	5 ± 7%	24 ± 4%	9 ± 6%
CPFM	5 ± 7%	14 ± 4%	7 ± 7%

material system. The standard deviations of the experimental results are depicted using error bars.

This presentation of the model predictions reveals some trends across the different approaches. All of the models under-predict the transverse tensile modulus with the models stepping closer the experimental results from ROM, ROMC, CCM, and CPFM (least to most accurate). The shear modulus is also under-predicted by all of the models, but with CCM and CPFM offering a steep improvement in accuracy relative to the ROM methods. The CPFM method provides a slight advantage in comparison to the CCM shear result. To highlight the model performances more exactly, the difference between the experimental result and the model predictions is quantified using

$$D = \frac{X_{exp.} - X_{mod.}}{X_{exp.}} \cdot 100\%, \tag{41}$$

where D represents the percent difference between the experimentally measured and modeled values of quantity X. The average of the differences for all material systems using each model are collected in Table 1, which represents an overall quantification of the accuracy for each model. The standard deviation of the predictions made with each method are provided to quantify the repeatability or robustness of each model

The axial tensile modulus approximations using all of the models are identical. The axial results demonstrate acceptable accuracy that is

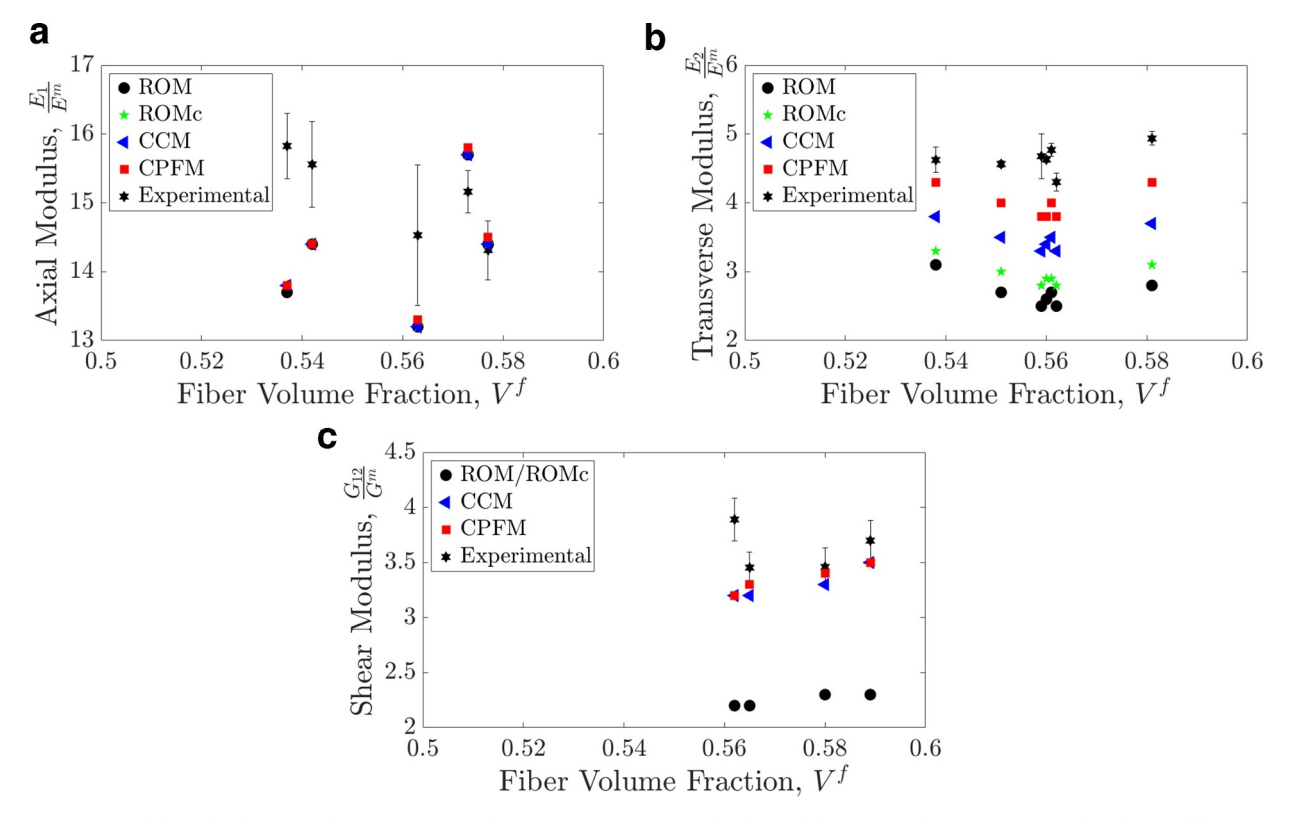


Fig. 1. Comparisons of the Rule of Mixtures basic (ROM), complex (ROMc), Composite Cylinder Model (CCM), and Continuous Periodic Fiber Model (CPFM) results with the experimental data for a) Axial tensile modulus E_1 b) Transverse tensile modulus E_2 and c) Axial shear modulus G_{12} , normalized by their resin moduli.

within the range of experimental repeatability (7%), however the standard deviation between material systems is fairly high. The transverse tensile modulus proves to be the most difficult to predict, with an average difference of 14% using CPFM to 41% using ROM. While the deviation of the CPFM result from average experimental value is greater than the desired accuracy range, it is substantially improved relative to the traditional models, where the next closest result was CCM at 24% difference. The CCM result is about 1.7 times further from the experiment than that of CPFM. Based on the standard deviations, all of the transverse models demonstrated better repeatability compared to that of the axial moduli. Using CPFM, the shear modulus can be approximated to the same accuracy level as the experimental data and it is marginally better than the results of CCM (7% difference versus 9%). However, the CPFM model has a high standard deviation (7%) from one material system to the next.

6. Conclusions

The Continuous Periodic Fiber Model (CPFM) presented in this work offers great promise and improved accuracy in comparison with the standard models used in practice, particularly for transverse properties of primarily uniaxial composites. The CLT calculations have overshadowed the shortcomings of traditional models in accurately predicting the transverse properties of uniaxial lamina, as the overall response of most engineering composites is heavily dominated by the properties in the fiber direction when they are not primarily uniaxial. Although the axial tensile and shear moduli were within the target accuracy range of 1-7% difference from experimental values, the transverse tensile modulus accuracy of 14% was greater than the desired range. Nevertheless, the model predicts composite performance with greater accuracy than previously achievable (e.g., 24% in CCM). This case of primarily uniaxial composites has gained in industrial relevance in recent years due to increasing wind turbine blade lengths that utilize nearly uniaxial skins, and whose transverse stiffness is clearly underestimated, yet relevant in many design aspects, such as their torsional rigidity and stability. Therefore, the more realistic values obtained by CFPM provides an opportunity for potential cost savings and weight reductions. While marked improvements in transverse values were achieved, the Continuous Periodic Fiber Model (CPFM) as presented here has room for improvement. Future work on the model may include changing the periodic unit cell geometry to reflect a hexagonal packed array, which generally provides a more realistic representation of the aligned fibers. The method could also be extended to predict the material strength along with its elastic properties. Models of material strength and composite failure would provide useful information regarding crack propagation and manufacturing related defects such as voids or weak bond lines.

Acknowledgments

This material is based upon work supported by the National Science

Foundation under Grant Number IIP-1362022 (Collaborative Research: I/UCRC for Wind Energy, Science, Technology, and Research). Any opinions, findings, and conclusions or recommendations expressed in this material are those of the authors and do not necessarily reflect the views of the National Science Foundation. The authors would like to thank the WindSTAR Company Members (Aquanis Inc., EDP Renewables, Bachmann Electronic Corp, GE Energy, Huntsman, Hexion, Leeward Asset Management LLC, Pattern Energy, TPI Composites Inc.) for funding this research.

The authors are extremely grateful to Steve Nolet and Tim Fallon from TPI Composites for providing the invaluable experimental data used in the model validation and for many insightful conversations. The authors also wish to thank Marc Chouinard and Hui Zhou from Huntsman for their input and dedicated support.

References

- Aboudi, J., 1996. Micromechanical analysis of composites by the method of cells update. Appl. Mech. Rev. 49 (10S), S83–S91. https://doi.org/10.1115/1.3101981.
- Christensen, R.M., Lo, K.H., 1979. Solutions for effective shear properties in three phase sphere and cylinder models. J. Mech. Phys. Solids 27 (4), 315–330. https://doi.org/ 10.1016/0022-5096(79)90032-2.
- Eder, M.A., Bitsche, R.D., 2015. Fracture analysis of adhesive joints in wind turbine blades. Wind Energy 18 (6), 1007–1022. https://doi.org/10.1002/we.1744.
- Eshelby, J.D., 1957. The determination of the elastic field of an ellipsoidal inclusion, and related problems. Proc. R. Soc. A 241 (1226), 376–396. https://doi.org/10.1098/rspa.1957.0133.
- Griffith, D.T., Ashwill, T.D., 2011. The sandia 100-meter all-glass baseline wind turbine blade: SNL100-00. Report No. SAND2011-3779. Sandia National Laboratories, Albuquerque.
- Hashin, Z., 1966. Viscoelastic fiber reinforced materials. AIAA J. 4 (8), 1411–1417. https://doi.org/10.2514/3.3686.
- Hill, R., 1963. Elastic properties of reinforced solids: some theoretical principles. J. Mech. Phys. Solids 11 (5), 357–372. https://doi.org/10.1016/0022-5096(63)90036-X.
- Hyer, M.W., 1998. Stress analysis of fiber-reinforced composite materials. WCB McGraw-
- Iwakuma, T., Nemat-Nasser, S., 1983. Composites with periodic microstructure. Comput. Struct. 16 (1), 13–19. https://doi.org/10.1016/0045-7949(83)90142-6.
- Luciano, R., Barbero, E.J., 1994. Formulas for the stiffness of composites with periodic microstructure. Int. J. Solids Struct. 31 (21), 2933–2944. https://doi.org/10.1016/ 0020-7683(94)90060-4.
- Mura, T., 1987. Micromechanics of defects in solids. M. Nijhoff.
- Nantasetphong, W., Amirkhizi, A.V., Jia, Z., Nemat-Nasser, S., 2016. Dynamic properties of polyurea-milled glass composites part II: micromechanical modeling. Mech. Mater. 98, 111–119. https://doi.org/10.1016/j.mechmat.2016.04.006.
 Nemat-Nasser, S., Hori, M., 1993. Micromechanics: overall properties of heterogeneous
- Nemat-Nasser, S., Hori, M., 1993. Micromechanics: overall properties of heterogeneous materials. Elsevier.
- Nemat-Nasser, S., Iwakuma, T., Hejazi, M., 1982. On composites with periodic structure. Mech. Mater. 1 (3), 239–267. https://doi.org/10.1016/0167-6636(82)90017-5.
- Reuss, A., 1929. Berechnung der fließgrenze von mischkristallen auf grund der plastizitätsbedingung fr einkristalle . ZAMM 9 (1), 49–58. https://doi.org/10.1002/ zamm 19290090104
- Schubel, P.J., Crossley, R.J., 2012. Wind turbine blade design. Energies 5 (9), 3425–3449. https://doi.org/10.3390/en5093425.
- Voigt, W., 1889. Ueber die beziehung zwischen den beiden elasticittsconstanten isotroper körper. Ann. Phys. 274 (12), 573–587. https://doi.org/10.1002/andp.18892741206.